Journal of Power Sources 196 (2011) 6293–6298

Contents lists available at ScienceDirect

Journal of Power Sources

journal homepage: www.elsevier.com/locate/jpowsour

One thousand-hour long term characteristics of a propane-fueled solid oxide fuel cell hot zone

Daan Cui, Yanhai Du*, Kenneth Reifsnider, Fanglin Chen

Solid Oxide Fuel Cells Center of Excellence, Department of Mechanical Engineering, University of South Carolina, Columbia, SC 29208, USA

ARTICLE INFO

Article history:
Received 15 February 2011
Received in revised form 30 March 2011
Accepted 31 March 2011
Available online 8 April 2011

Keywords:
Solid oxide fuel cell
Long term durability test
Propane-fueled
Self-sustained hot zone
Degradation

ABSTRACT

One thousand-hour continuous test of a propane-fueled portable solid oxide fuel cell (SOFC) based hot zone has been successfully performed in order to assess the degradation characteristics of its performance. Comparing the different operating modes, the degradation rate based on constant current mode was three times lower than that based on constant voltage mode. The stack power output initially increased 3.7% during the first 34 h probably due to electrode activation processes improving cell performance under polarization during the early stage of operation, and then gradually decreased. It has been clearly illustrated that operating condition of constant current is more beneficial to the long term performance test. Further, based on thermodynamics analysis, the electromotive force of nickel oxidation is 13.2 V for the stack voltage at the stack temperature of 740 °C. From the initial current–power curve data, it can be derived that if the hot zone durability test was performed at constant current of 9 A from the beginning, the stack degradation rate would be 15% per 1000 h. The 1000-h durability test and analysis can better understand how to run longer term stability on the hot zone and guide the optimization of hot zone operating conditions.

1. Introduction

With the depletion of the fossil energy resources and the increasingly global environmental concerns, high efficiency and environmental-friendly technologies for electricity generation are becoming an intensive demand. Solid oxide fuel cells (SOFCs) based on ceramic electrolytes can be fabricated with cost effective materials for catalysts, electrolytes, interconnects and other structural components [1–6]. Moreover, SOFCs are fuel flexible and can be operated on H_2, CO, gasified coal gas, and short chain hydrocarbons. Due to these advantages [7], there are several promising SOFC applications, such as auxiliary power units (APUs) and residential power generators. Recently, portable SOFC applications have been extensively studied [4,5,8].

Of the fuel choices available for portable fuel cell power applications, propane is particularly attractive because it is widely available and has a sufficiently high vapor pressure, and can also be readily stored with high energy density at room temperature (46.4 MJ kg^{-1}) as a liquid phase under moderate pressure (ca.10 atm at room temperature), being considerably much higher than that for methanol (19.9 MJ kg^{-1}) [9–15]. Consequently, propane-fueled SOFC portable generators have significant advantages over direct methanol polymer electrolyte membrane fuel cell (PEMFC) generators.

Long-term stability is an important requirement for the SOFC application. The total performance degradation rate of the SOFC hot zone under constant operating conditions is the sum of contributions from all components, including anode, cathode, electrolyte of the cell, sealing, as well as auxiliary components [16,17]. For cell components, many degradation mechanisms have been discussed in literatures, such as the enrichment of impurities at the three-phase boundary [18], high resistive layers produced by reactions between components, the failure of the anode caused by carbon deposition or sulfur poisoning when directly using hydrocarbons as fuel, the coarsening of Ni particles [19,20], Cr poisoning at the cathode side caused by the Cr in interconnects, changes of the microstructure in the cathode [21] and delamination caused by thermal stress continuously generated due to differences in thermal expansion coefficients (TECs) of neighboring cell layers. Besides degradation, initial activation processes leading to cell performance enhancement could also overlap with the degradation under polarization, resulting in more difficultly in evaluating reliability. The operating conditions also affect these mechanisms differently. However, the reliability of high performance SOFC hot zone must be better understood in order to effectively develop and deploy SOFCs as power sources. Despite efforts from many research groups to study performance on single cells, it is very difficult to guarantee reliability because of including many complex issues

* Corresponding author. Tel.: +1 803 777 4133.
E-mail address: duya@engr.sc.edu (Y. Du).

0378-7753/$ – see front matter © 2011 Elsevier B.V. All rights reserved.
doi:10.1016/j.jpowsour.2011.03.098

[7,22–24]. Achieving reliability for portable applications of SOFCs during long-term operation is necessary due to lack of available reports on this topic in the literature.

In the present study, 1000-h long-term characteristics of a propane-fueled and thermally self-sustained SOFC hot zone tested under constant operating conditions have been evaluated as a function of hot zone temperatures, currents and voltages. Degradation rates are evaluated under corresponding operating conditions. The objective of this work is to establish some general degradation mechanisms for a propane-fueled and thermally self-sustained SOFC hot zone.

2. Experimental

A test station (500 W) from TesSol® was configured and employed for evaluating the fuel cell hot zone performance. The compact 500 W test stand with load bank, fuel and gas delivery units, six temperature monitoring channels and data acquisition software was utilized to evaluate stack and record data. A 95-lb. cylinder with instrument-grade propane (99.5%) ordered from Airgas was utilized for all the tests. No sulfur was present in the 95-lb. cylinder according to the analytical results provided by the vendor. Impurities of the propane were carbon dioxide (1 ppm), oxygen (5 ppm), nitrogen (1 ppm), propylene (46 ppm), other hydrocarbons (638 ppm) and water (3 ppm). The compressed Air was filtered prior to introducing to cathode and anode in the hot zone testing.

Due to direct utilization of higher hydrocarbons (e.g. propane) as the fuel in SOFCs having caused severe carbon deposition and rapid deactivation of electrode, hydrocarbon-fueled SOFC systems will therefore require a fuel processing system, such as steam reforming and partial oxidation, converting hydrocarbons to a mixture of hydrogen and carbon monoxide prior to feeding to SOFC stacks and effectively avoiding carbon deposition. The catalytic partial oxidation (CPOX) utilized in the present hot zone was the most suitable for portable power applications. In this case, when a stream of propane is mixed with an air stream, the following reaction would take place:

$$C_3H_8 + 1.5O_2 + 6N_2 \rightarrow 4H_2 + 3CO + 6N_2 \quad (1)$$

The hot zone consisted of the stack, catalyst reformer unit, tail gas combustor (TGC) and thermal insulations. The stack was assembled from 18 micro-tubular SOFCs (nickel-based and anode-supported) in a serial connection. A CPOX reformer was integrated into the hot zone to reform the propane fuel. The reformate fuel contained approximately 29% H_2 and 21% CO. At initial startup, the fuel was combusted together with the gas from the cathode in TGC. The heat produced in the flue gas stream was utilized to pre-heat the inlet air and the hot zone to reach the appointed temperature during start-up.

Unless where they are specified, the following operating conditions were applied for evaluating the hot zone. Fuel flow: C_3H_8 of 0.43 SLPM with CPOX air of 3.45 SLPM; cathode air flow: 16 SLPM. The hot zone was characterized in a hood, including start up, voltage–current/power (IV/IP) curve determination at different running terms and 1000 h long term test.

3. Results and discussion

3.1. Characteristics of hot zone startup and initial performances

The hot zone was tested in the hood. First, it was started up by lighting the fuels to generate the initial heat needed to warm up the catalyst reformer. Once the CPOX reactor reached the working temperature, the heat from exothermic catalytic reactions plus the heat from exhaust combustions would provide sufficient heat to keep the hot zone thermally self-sustained. The operating parameters such as O/C ratio and air flow rate could be adjusted in order for the stack temperature to be stable at the desired point.

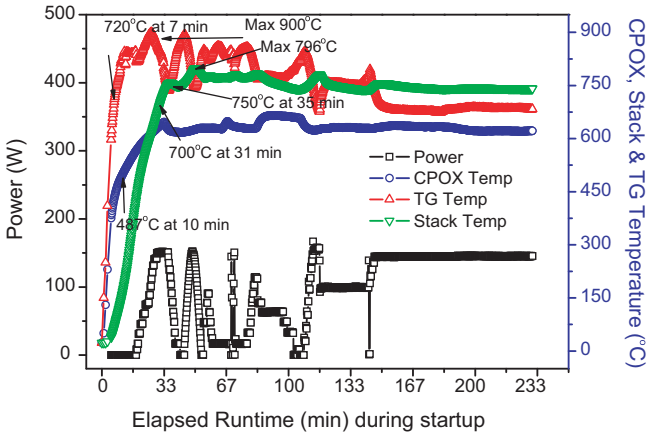

Fig. 1. Hot zone performance and CPOX, stack & TGC temperature in hot zone fueled by C_3H_8 during startup.

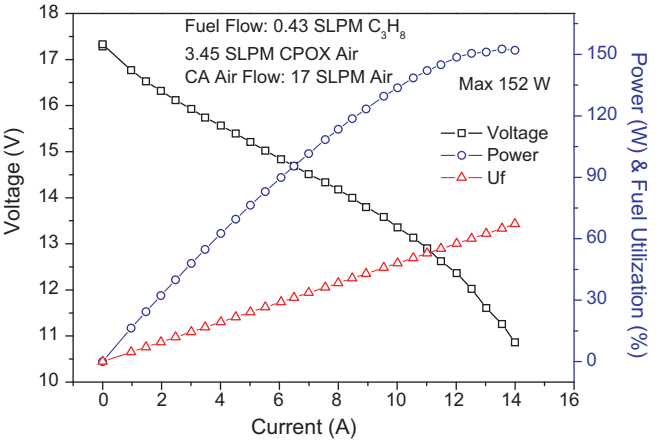

Fig. 2. Performance of hot zone at the 50th min, C_3H_8 of 0.43 SLPM with air of 3.45 SLPM for fuel and cathode air flow rate 17 SLPM for oxidant.

The hot zone was successfully tested on its startup characteristics and initial IV/IP performance characteristics. The characteristics of the hot zone at the startup stage were shown in Fig. 1, including the CPOX, stack and TGC temperature variations during startup. The startup characteristics of the hot zone were observed as: the TGC temperature increased to over 720 °C within 7 min; 10 min were needed for the CPOX temperature to reach 487 °C; and the stack temperature rose gradually to 700 °C within 31 min. The operating voltage was set close to open circuit voltage during the start-up. In the beginning stage, the IV and IP performance were obtained. The fluctuations until 150 min were caused due to the stack performance testing.

After the stack temperature was stabilized around 740 °C, VI/VP performance curves were conducted at the 50th min and the 70th min. Performance characteristics of the hot zone at the 50th min and the 70th min were shown in Figs. 2 and 3, respectively. The operating conditions for the hot zone performance test were similar: fuel flow for them was both C_3H_8 of 0.43 SLPM with air of 3.45 SLPM for CPOX reaction; cathode air flow rate was 17 SLPM for the 50th min test and 21 SLPM for the 70th min test. The maximum output powers of the hot zones were 152 W and 157 W for the two tests, respectively. The fuel utilization referred to reformate

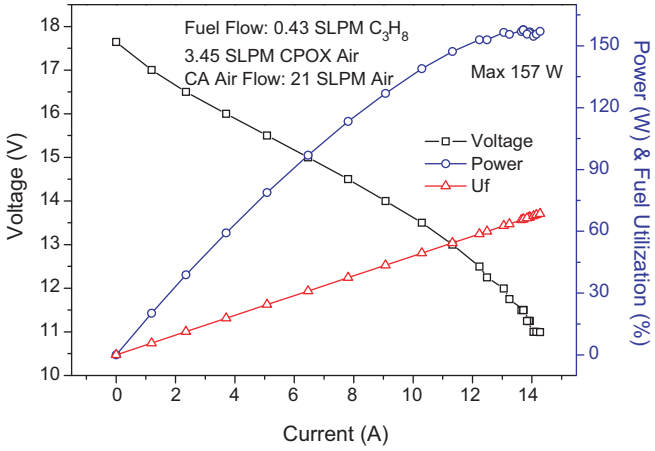

Fig. 3. Performance of hot zone at the 70th min, C_3H_8 of 0.43 SLPM with air of 3.45 SLPM for fuel and cathode air flow rate 21 SLPM for oxidant.

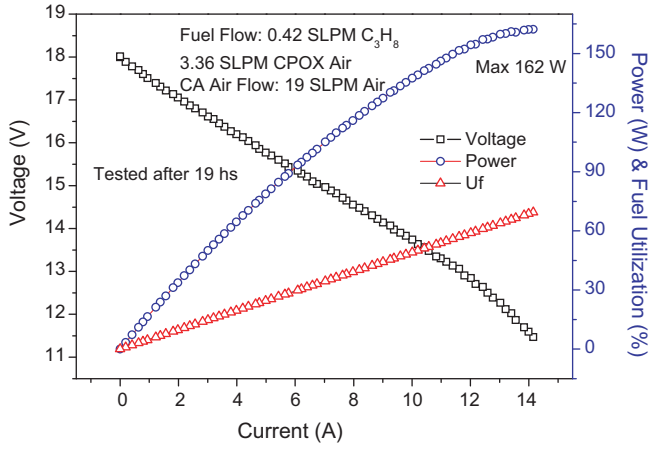

Fig. 4. Performance of hot zone tested at the 19th h, C_3H_8 of 0.42 SLPM with air of 3.36 SLPM for fuel and cathode air flow rate 19 SLPM for oxidant.

utilization:

$$\text{OC-Ratio} = \frac{\text{Air Fuel flow} \times 0.42}{(3 \times \text{Propane flow})} = \frac{0.14 \times \text{Air Fuel flow}}{\text{Propane flow}} \quad (2)$$

At 20 °C of the environmental temperature

$$U_f = \text{Current} \times 18 \times 7.6/((10 - 3 \times \text{OC-Ratio}) \times \text{Propane flow} \times 1000) \quad (3)$$

The maximum fuel utilizations were over 60% for them. The temperatures at stable operating conditions were 740 °C (stacks), 620 °C (CPOX) and 690 °C (TGC). The performance at the 70th min was slight higher than that at the 50th min. Although the hot zone temperature was stable, the SOFC stack performance still increased slightly. It illustrated that activation processes improving cell performance occurred under polarization during the initial stage.

3.2. One thousand-hour long term characteristics of hot zone

After performance tests at startup, 1000-h long-term durability on performance was evaluated. The long-term stability was evaluated under constant currents (11 A or 9 A), as shown in Figs. 4–11. The 1000-h continuous test was achieved. The IV/IP performance of hot zone for long term test was evaluated at the 19th h, the 100th h and the 240th h according to the following operating conditions: C_3H_8 fuel flow was 0.42 SLPM with air of 3.36 SLPM for the CPOX reaction and cathode air flow rate was 19 SLPM. The results for

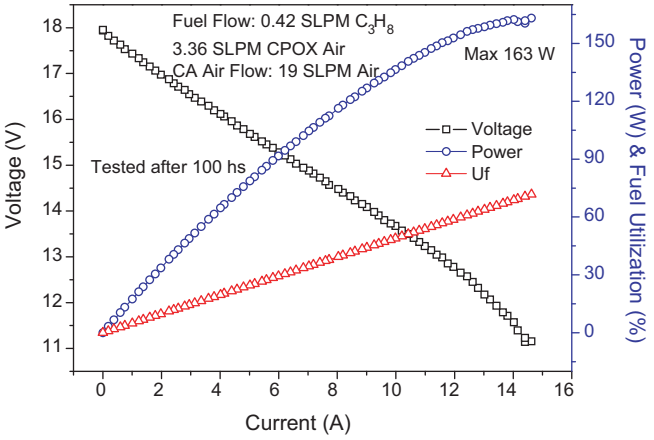

Fig. 5. Performance of hot zone at the 100th h, C_3H_8 of 0.42 SLPM with air of 3.36 SLPM for fuel and air flow rate 19 SLPM for oxidant.

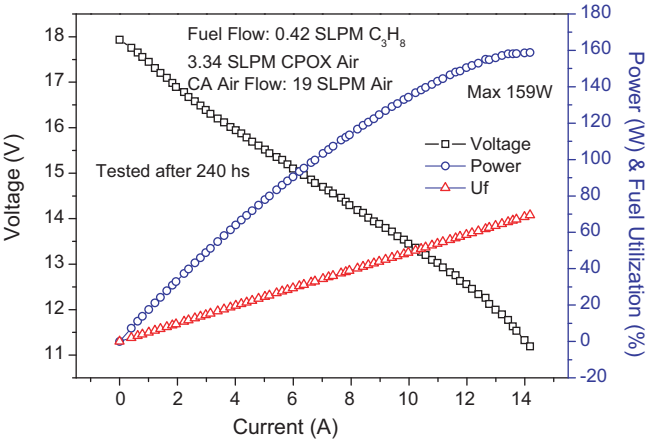

Fig. 6. Performance of hot zone at the 240th h, C_3H_8 of 0.42 SLPM with air of 3.36 SLPM for fuel and air flow rate 19 SLPM for oxidant.

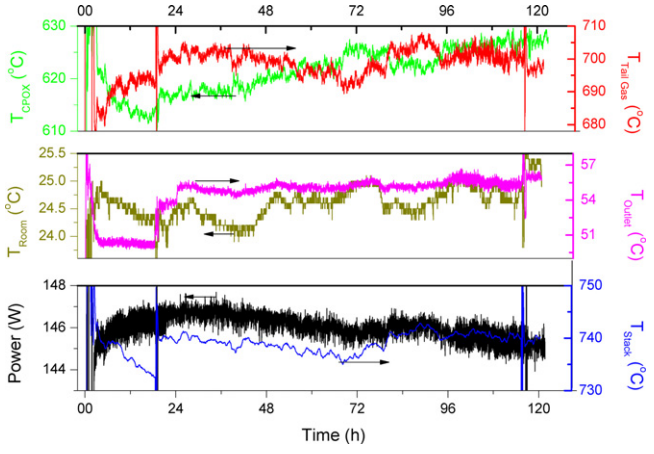

Fig. 7. Hot zone performances, stack, CPOX, TGC, outlet of hot zone and room temperatures for 120 h operation, C_3H_8 flow of 0.42 SLPM with CPOX air of 3.36 SLPM for fuel and air of 19 SLPM for oxidant.

performance tests at the 19th h, the 100th h and the 240th h were shown in Figs. 4–6. The maximum power outputs at the 19th h, the 100th h and the 240th h were 162 W, 163 W and 159 W, respectively.

Fig. 7 showed the hot zone performance, stack, CPOX, TGC, outlet of hot zone and room temperatures during the first 120 h operation. The stack temperature was held at about 740 °C during the

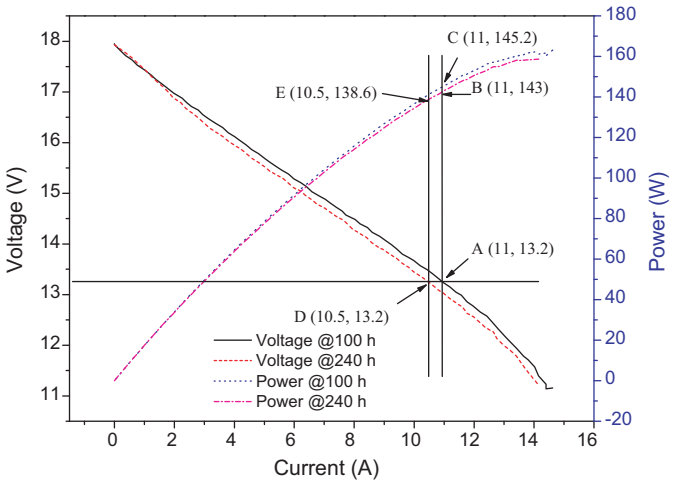

Fig. 8. Performance analysis of hot zone at the 100th h and the 240th h.

first 120 h operation, without changing operating conditions (C_3H_8 of 0.42 SLPM with 3.36 SLPM CPOX air for fuel flow and air of 19 SLPM for cathode oxidant). From Fig. 7, it was found that operating temperatures of all components were fluctuating with time. The room temperature has variations during the day and night alternation. When the room temperature decreased, it was found that the CPOX temperature also deceased and TGC temperature increased. Moreover, the variations of CPOX temperature and TGC temperature showed opposite trends during the overall testing process. Meanwhile, both the stack power and stack temperature showed the similar trend with the variation of TGC temperature after the 19th h, i.e., higher stack temperature resulting in higher stack performance. During the first 19 h, the CPOX and stack temperatures were both decreasing as a function of the operating time. This might be due to the fact that the fan of the hood stopped working during stack operation, causing a reduction in oxygen intake to the CPOX in hot zone, and consequently decreasing the CPOX temperature.

Fig. 8 showed the performance analysis of hot zone at the 100th h and the 240th h. From Fig. 8, the different operating modes including constant current and constant voltage were compared for the evaluation of the degradation behaviors of the stack. Points A and D showed the current values under the same stack voltage for the two tests. The stack currents were 11 A at 100 h and 10.5 A at 240 h under same stack voltage of 13.2 V based on the two IV curves. Points C and E showed the power values under the same stack voltage of 13.2 V. The degradation according to the constant stack voltage was 32.5% per 1000 h. Points C and B showed the power values under the same stack current of 11 A, 145.2 W for testing at the 100th h and 143 W for testing at the 240th h. The degradation according to constant stack current was 10.8% per 1000 h. The results illustrated that the degradation based on constant current mode was three times lower than that using constant voltage operating mode. Moreover, the constant current mode can readily maintain consistent fuel utilization and uniform reaction conditions nearby triple phase boundaries of the anode.

Fig. 9 showed the hot zone performance and the stack temperature of 1000 h long term test. Fig. 10 further showed the detailed analysis for hot zone durability tests. The stack power initially increased 3.7% during the first 34 h due to activation processes improving cell performance under polarization, and then gradually decreased at a rate of 1.7% per 100 h till the 313th h at constant current of 11 A. Because of the unpredicted sharp performance drop afterwards, the operating current was changed from 11 A to 9 A at the 331th h to avoid the oxidation of nickel under low operating voltage. Fig. 11 showed the load change at the 331th h, where the stack current was changed from 11 A to 9 A. Moreover, holding at a constant voltage mode of 13.2 V produced a sharp degradation of 207% per 100 h at the 331th h. Therefore, the constant current mode was still chosen for the remaining long term test. It clearly illustrates that constant current operating condition is more beneficial to long term test.

To further understand nickel oxidation under low operating voltages from thermodynamics point of view, plotted in Fig. 12 is the electromotive force of nickel oxidation (E_{Ni}) representing the Ni–NiO equilibrium, below which the oxidation of Ni taking place. E_{Ni} was calculated based on Eqs. (4) and (5). Due to solid Ni and NiO, the E_{Ni} is only dependent on T when fixing oxidant such as ambient P_{O_2} (0.21 atm), but independent on P_{H_2}. It can be seen that the cell voltage for nickel oxidation becomes invariant in an SOFC. From Eq. (5), it was concluded that E_{Ni} was 0.73 V for a single cell (13.2 V for the stack voltage) at stack temperature of 740 °C. When stack voltage was below 13.2 V, Ni might be oxidized based on the above analysis. Therefore, the operating condition was adjusted when the stack voltage reached 13.2 V.

$$\mathrm{Ni(s)} + 1/2\mathrm{O_2(g)} = NiO(s)$$
$$\Delta G^{\circ} = -234,122 + 85.15 \times T\ (298\text{–}1725\ \mathrm{K}) \quad (4)$$

$$E_{\mathrm{Ni}}(\mathrm{V}) = 1.2132 - 4.7487 \times 10^{-4} \times T(\mathrm{K}) \quad (5)$$

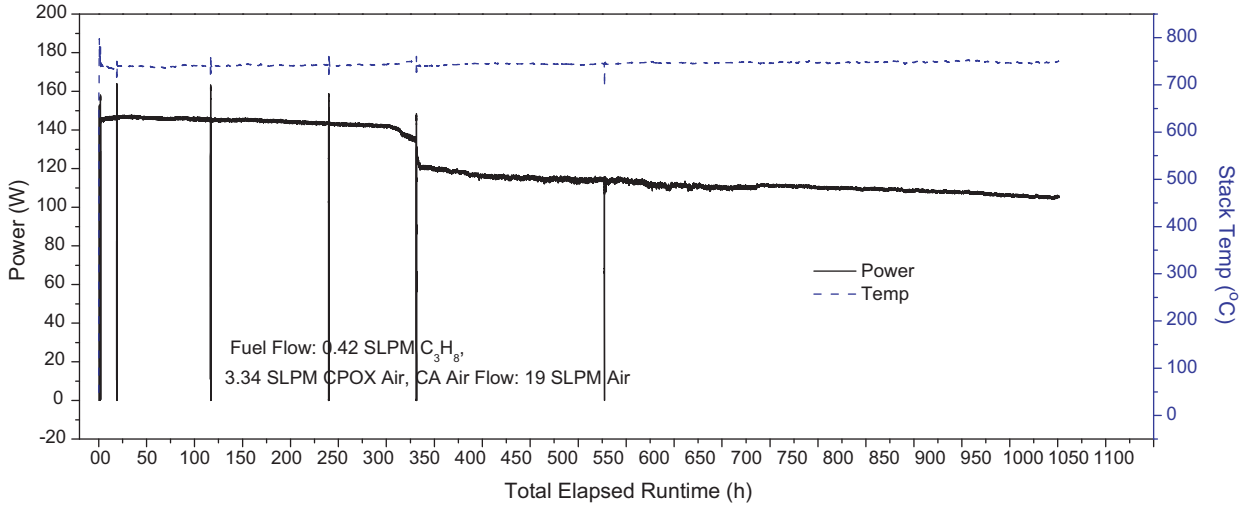

Fig. 9. Hot zone performance and stack temperature of 1000 h long term test.

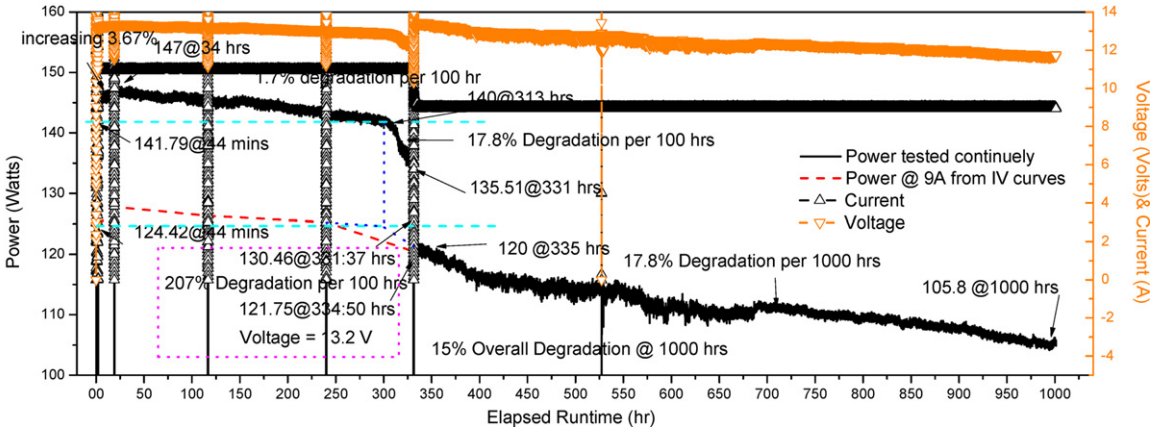

Fig. 10. Detailed analyses for hot zone durability.

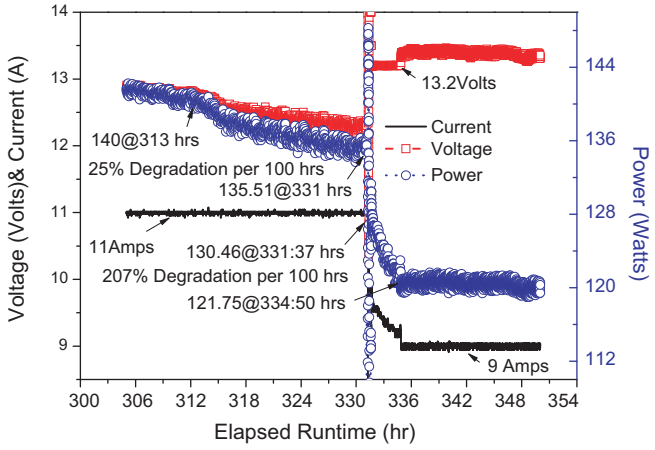

Fig. 11. Load change at the 331th h.

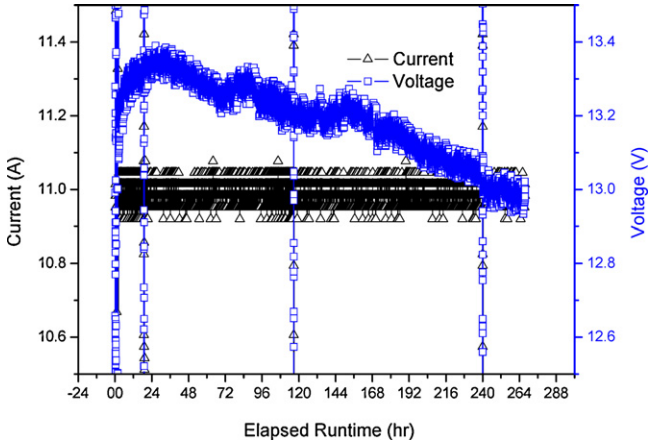

Fig. 13. Effect of load bank on current and voltage.

After reducing the stack operating current from 11 A to 9 A, the stack performance degraded at a rate of 17% per 1000 h until reaching 1000 h operating time. From the initial current–power curve data, 124.42 W at 9 A, and the power of 105.8 W at the 1000th h at 9 A, it can be estimated that if the durability test was operated at constant current of 9 A from the beginning, the stack degradation rate would be (124.42–105.8)/124.42 = 15% per 1000 h.

From Fig. 7, a relative wide line for the recorded power can be found. Therefore, the effect of load bank on the recorded currents and voltages was also investigated. Fig. 13 showed the effect of load bank on currents and voltages. When current was set at 11 A, the current value can be changed between 11.05 A and 10.93 A. The changing value was 0.12/11 = 1.1%. For voltages, the fluctuated range was 0.045/13.3 = 0.34% when the value was close to 13.3 V.

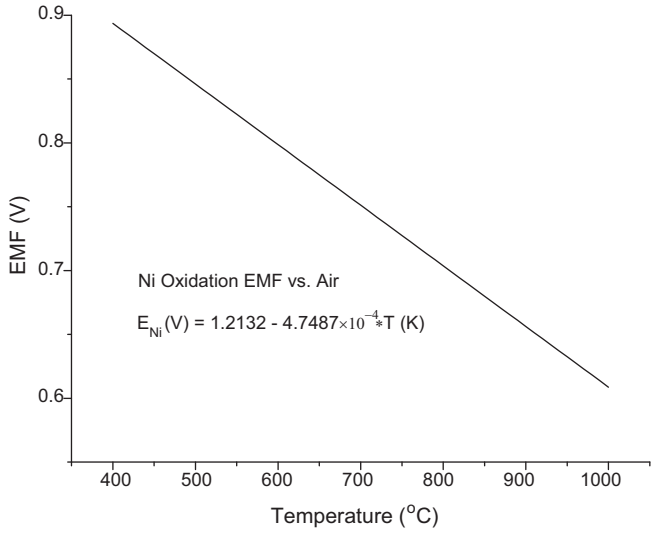

Fig. 12. Variations of electromotive force of Ni oxidation (E_{Ni}) with temperature variation.

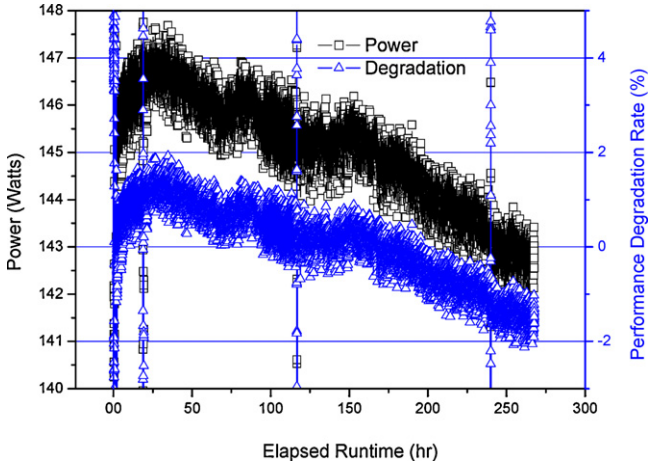

Fig. 14. Effect of load bank on power.

Fig. 14 showed the effect of load bank on power setting and the changing range was 1/147 = 0.68%. According to the above analysis for load bank, the fluctuating current from load bank caused the power variation.

4. Conclusions

A portable SOFC-based hot zone producing maximum 163 W of electric power from propane was successfully demonstrated and evaluated for startup, VI/VP characteristics and 1000-h continuous test of long term durability. Based on thermodynamics analysis, the electromotive force of nickel oxidation is 13.2 V for the stack voltage at stack temperature of 740 °C. Comparing different evaluating modes for the stack, the degradation rate based on constant current mode was three times lower than that using constant voltage mode. The stack power initially increased 3.7% during the first 34 h due to activation processes improving cell performance under polarization, and then gradually decreased at a rate of 1.7% per 100 h until the 313th h at a constant current of 11 A. From the initial current–power performance data, it can be derived that if operating the durability from the beginning at a constant current of 9 A, the stack degradation rate would be 15% per 1000 h. It has been clearly illustrated that operating condition of constant current was more beneficial to long term test. The 1000-h long term test and analysis can help understand how to run longer term stability on thermally self-sustained hot zone employing a propane-powered SOFC as a core component, and offers guidance in the optimization of hot zone operating conditions in the portable system.

Acknowledgment

University of South Carolina would like to acknowledge the financial support of the United States DARPA under contract ARL001-007.

References

[1] K. Huang, J.B. Goodenough, Solid Oxide Fuel Cell Technology: Principles Performance and Operations, Woodhead Publishing, Cambridge, 2009.
[2] Z. Zhan, S.A. Barnett, Science 308 (2005) 844–847.
[3] T. Suzuki, Z. Hasan, Y. Funahashi, T. Yamaguchi, Y. Fujishiro, M. Awano, Science 325 (2009) 852–855.
[4] Z. Shao, S.M. Haile, J. Ahn, P.D. Ronney, Z. Zhan, S.A. Barnett, Nature 435 (2005) 795–798.
[5] P.K. Cheekatamarla, C.M. Finnerty, C.R. Robinson, S.M. Andrews, J.A. Brodie, Y. Lu, P.G. DeWald, J. Power Sources 193 (2009) 797–803.
[6] D. Cui, L. Liu, Y. Dong, M. Cheng, J. Power Sources 174 (2007) 246–254.
[7] K. Park, S. Yu, J. Bae, H. Kim, Y. Ko, Int. J. Hydrogen Energy 35 (2010) 8670–8677.
[8] P.K. Cheekatamarla, C.M. Finnerty, Y. Du, J. Jiang, J. Dong, P.G. Dewald, C.R. Robinson, J. Power Sources 188 (2009) 521–526.
[9] Z. Zhan, S.A. Barnett, Solid State Ionics 176 (2005) 871–879.
[10] M.L. Faro, D.L. Rosa, G. Monforte, V. Antonucci, A.S. Arico, P. Antonucci, J. Appl. Electrochem. 37 (2007) 203–208.
[11] Z. Zhan, J. Liu, S.A. Barnett, Appl. Catal. A: Gen. 262 (2004) 255–259.
[12] V. Modafferi, G. Panzera, V. Baglio, F. Frusteri, P.L. Antonucci, Appl. Catal. A: Gen. 334 (2008) 1–9.
[13] K. Fo1ger, K. Ahmed, J. Phys. Chem. B 109 (2005) 2149–2154.
[14] J. Liu, B.D. Madsen, Z. Ji, S.A. Barnett, Electrochem. Solid-State Lett. 5 (2002) A122–A124.
[15] S. McIntosh, J.M. Vohs, R.J. Gorte, J. Electrochem. Soc. 150 (2003) A470–476.
[16] S.P. Simner, M.D. Anderson, L.R. Pederson, J.W. Stevenson, J. Electrochem. Soc. 152 (2005) A1851–A1859.
[17] A. Hagen, R. Barfod, P.V. Hendriksen, Y. Liu, S. Ramousse, J. Electrochem. Soc. 153 (2006) A1165–A1171.
[18] Y.L. Liu, S. Primdahl, M. Mogensen, Solid State Ionics 161 (2003) 1–10.
[19] D. Skarmoutsos, F. Tietz, P. Nikolopoulos, Fuel Cells 1 (2001) 243–248.
[20] A. Ioselevich, A.A. Kornyshev, W. Lehnert, Solid State Ionics 124 (1999) 221–237.
[21] S.P. Jiang, W. Wang, Solid State Ionics 176 (2005) 1185–1191.
[22] A. Hagen, K. Neufeld, Y.L. Liu, J. Electrochem. Soc. 157 (2010) B1343–B1348.
[23] J. Nielsen, A. Hagen, Y.L. Liu, Solid State Ionics 181 (2010) 517–524.
[24] F. Calise, G. Restucccia, N. Sammes, J. Power Sources 196 (2011) 301–312.